Effects of ultrasound on the degradation kinetics, physicochemical properties and prebiotic activity of *Flammulina velutipes* polysaccharide

Jinrong Xiao [a], Xin Chen [a], Qiping Zhan [a], Lei Zhong [a], Qiuhui Hu [a,b], Liyan Zhao [a,*]

[a] *College of Food Science and Technology, Nanjing Agricultural University, Nanjing, China*
[b] *College of Food Science and Engineering, Nanjing University of Finance and Economics, Nanjing, China*

ARTICLE INFO

ABSTRACT

The controllable ultrasonic modification was hindered due to the uncertainty of the relationship between ultrasonic parameters and polysaccharide quality. In this study, the ultrasonic degradation process was established with kinetics. The physicochemical properties and prebiotic activity of ultrasonic degraded *Flammulina velutipes* polysaccharides (U-FVPs) were investigated. The results showed that the ultrasonic degradation kinetic models were fitted to $1/M_t - 1/M_0 = kt$. When the ultrasonic intensity increased from 531 to 3185 W/cm^2, the degradation proceeded faster. The decrease of polysaccharide concentration contributed to the degradation of FVP, and the fastest degradation rate was at 60 °C. Ultrasound changed the solution conformation of FVP, and partially destroyed the stability of the triple helix structure of FVP. Additionally, the viscosity and gel strength of FVP decreased, but its thermal stability was improved by ultrasound. Higher ultrasonic intensity led to larger variations in physicochemical properties. Compared with FVP, U-FVPs could be more easily utilized by gut microbiota. U-FVPs displayed better prebiotic activity by promoting the growth of *Bifidobacterium* and *Brautella* and inhibiting the growth of harmful bacteria. Ultrasound could be effectively applied to the degradation of FVP to improve its physicochemical properties and bioactivities.

1. Introduction

Flammulina velutipes, the fourth largest edible fungus in the world, is widely distributed in Asia, North America, Australia and other countries or regions. Especially in China, it has been used as a restorative drug and a tonic food as well [1]. Polysaccharide is the most abundant bioactive component in *Flammulina velutipes*. *Flammulina velutipes* polysaccharide (FVP) have been found to possess a variety of functions, including immuno-enhancement, lowering cholesterol and memory improvement [2–4]. Therefore, there are great potentials for FVP to be deeper investigated into functional foods. Notably, FVP was not degraded under the saliva-gastrointestinal digestion conditions, but could be consumed by human fecal microorganisms [5]. *In vivo* experiments have shown FVP possesses prebiotic properties. FVP achieved immune regulation and improvement of learning and memory impairment by regulating intestinal flora structure, with the changes in the abundance of *Lactobacillus*, *Bacteroidia*, *Erysipelotrichia* and *Clostridia* [3,4]. However, the application of FVP has been confined due to its high molecular weight (Mw) and viscosity. These shortcomings also delay the transport and absorption of FVP in the gastrointestinal system [6].

The physicochemical properties and functional activities of polysaccharides mainly depend on their molecular structure, including Mw, branching degree, conformation and so on [7]. Numerous pieces of evidence have shown that the partially degraded polysaccharides with low Mw had good solubility and lower viscosity. Their functional groups were not changed, but their bioactivities were improved [8]. Furthermore, the modified physicochemical properties could affect the bioavailability of polysaccharides to human gut microbiota.

At present, there are mainly three kinds of degradation methods of polysaccharides: physical modification, chemical modification and biological modification. The shortcomings of chemical modification are the extensive use of organic reagents and the risk of chemical pollution [9]. Biological modification is a complex method, and its application is limited by the high cost [10]. As a new physical degradation technology of polysaccharides, there are many advantages of ultrasonic degradation, such as simple equipment, convenient operation, easy automation, and no pollution to the environment [11]. Ultrasonic degradation could not only effectively improve the physicochemical properties of polysaccharides, but also enhance their bioactivities such as anti-oxidation, anti-cancer, anti-inflammatory and hypoglycemic [12–14].

---

* Corresponding author at: College of Food Science and Technology, Nanjing Agricultural University, Nanjing 210095, China.
  E-mail address: zhlychen@njau.edu.cn (L. Zhao).

Nevertheless, to date, there was little information on the prebiotic activity of polysaccharides after ultrasonic degradation. Furthermore, the controllable ultrasonic modification was limited due to the uncertainty of the relationship between ultrasonic parameters and polysaccharide quality. And to our knowledge, there is no study on the effects of ultrasonic degradation on the physicochemical properties and bioactivities of FVP.

In order to achieve controlled ultrasonic degradation of FVP and improve its physicochemical properties and bioactivities, the kinetics of FVP ultrasonic degradation was fitted by the 0 order, 1st order and 2nd order kinetic models for the first time. Moreover, the effects of ultrasonic modification on the physicochemical properties and prebiotic activity of FVP were firstly clarified. This research will fill the gap in the field of controllable ultrasonic degradation technology of FVP, promoting the application of ultrasonic degradation for improving the prebiotic activity of polysaccharides in functional food.

2. Materials and methods

2.1. Materials and reagents

Fresh fruiting bodies of *Flammulina velutipes* were acquired from Jiangsu Jiangnan Biotechnology Co., Ltd. (Danyang, China). FVP samples were prepared according to the method reported by Chen et al [15]. T-series dextran (T-10, T-40, T-70, and T-2000), acetic, propionic, *n*-butyric, *i*-butyric, *n*-valeric, *i*-valeric and L-lactic acid were obtained from Sigma-Aldrich (St. Louis, Missouri, USA). Pancreatin, gastric lipase, bile salts, pepsin, trypsin, L-rhamnose (Rha), D-xylose (Xyl), D-glucuronic acid (GlcA), D-glucose (Glc), D-fructose (Fru), D-fucose (Fuc) and D-mannose (Man) were purchased from Shanghai Yuanye Biotechnology Co., Ltd (Shanghai, China). Insulin was purchased from Ryon (Shanghai, China). All the other chemical reagents were of analytical grade.

2.2. Ultrasonic degradation

Polysaccharide solution was sonicated at 20 kHz using an ultrasonic generator (JOYN-3000A, Qiaoyue Electronics Co. Ltd., Shanghai, China). An ultrasound probe with a 6 mm diameter was immersed into the solution with a fixed depth of 2 cm. The FVP solution (50 mL) was put into a reaction vessel (a 100 mL glass beaker). Then the beaker was held in the ultrasonic reactor and treated intermittently (1 s on, 2 s off). Ultrasonic degraded samples were prepared in three replicates. Effects on the ultrasonic degradation measured in the present work were arranged in Table 1.

The ultrasonic intensity was calculated based on the following formula [16]:

$$I = P/(\pi r^2) \tag{1}$$

where I is the ultrasonic intensity (W/cm²); P is the input ultrasonic power (W); and r is the radius of the probe tip (cm). In this study, the ultrasonic powers were set at 150, 300, 450, 600 and 900 W, which corresponded to ultrasonic intensities of around 531, 1062, 1592, 2123,

Table 1
Experimental design of ultrasonic degradation.

Experimental group[a]	Group 1	Group 2	Group 3
Ultrasonic intensities (W/cm)	531, 1062, 1592, 2123, 2654, 3185	2123	2123
Ultrasonic temperatures (°C)	60	0, 20, 40, 60, 80	60
Polysaccharide concentration (mg/mL)	4	4	2, 4, 6, 8, 10

[a] Groups G1 − G3 were for studying the effects of ultrasonic intensity, ultrasonic temperature and polysaccharide concentration on the degradation of FVP, respectively.

2654 and 3185 W/cm², respectively.

2.3. Molecular weight measurement

The average M_W was determined according to the previous research [15]. The HPLC system (1200, Agilent Technologies, United States) equipped with an evaporative light scattering detector (ELSD) was applied. The liquid chromatographic condition was shown in Supplementary Materials Table S1.

2.4. Degradation kinetics model

The degradation behavior of FVP under different ultrasonic modifications was described by the 0 order, 1st order and 2nd order reaction kinetics models, and the rate constant (k) was derived from the following formulas [16]:

$$Mt - M_0 = k_0 t \tag{2}$$

$$\ln(M_t/M_0) = k_1 t \tag{3}$$

$$1/M_t - 1/M_0 = k_2 t \tag{4}$$

where k_0 is the 0 order kinetic rate constant; k_1 is the 1st-order kinetic rate constant, (min^{-1}); k_2 is the 2nd order kinetic rate constant (mol·g^{-1}·min^{-1}); t is the treatment time (min); M_t and M_0 are the weight-average Mw at time t and at time 0 (g/mol), respectively.

2.5. Chemical composition analysis

Total sugar content was quantitatively determined using the phenol-sulfuric acid means [17]. Uronic acid content was estimated by the carbazole-sulfuric acid method [18]. Protein content was detected through the Coomassie brilliant blue method [18].

2.6. Measurement of particle size and ζ-potential

The particle size and ζ-potential were analyzed by dynamic light scattering (DLS) on a Zetasizer (Nano-S90, Malvern Instruments Ltd., Malvern, UK) at 632.80 nm and 90° scattering angle of 25 °C. The sample was prepared into a solution with a concentration of 0.2 mg/mL. The refractive indices of the dispersed phase and continuous phase were 1.414 and 1.330, respectively. Three runs were performed for each sample.

2.7. Rheological analysis

The steady shear rheology and dynamic oscillatory rheological properties of the sample solutions (5 % w/w) were determined by a rheometer (MCR302, Anton Paar, Graz, Austria) (probe: PP50/TG). The gap of the parallel plate was set at 60 μm [19]. The shear rate was set in the range of 0.1–400 s^{-1}. The storage modulus (G') and loss modulus (G'') were determined at oscillation frequency from 0.1 to 100 rad/s. All the experiments were performed at 25 ± 0.1 °C.

2.8. Conformation analysis

I_2-KI analysis and Congo red analysis of FVPs were performed with common methods [12,20], and the Circular dichroism (CD) spectra of FVPs was referenced Jaton's method [21]. Details were described in the supplement.

2.9. Thermal properties analysis

The thermal properties were measured with a DSC-60 Plus (Shimadzu Corporation, Kyoto, Japan). The dried sample (5 mg) was placed in an aluminum pan. Then polysaccharide was scanned and heated from

25 to 500 °C under N_2 atmosphere. The heating rate was 10 °C/min.

2.10. Crystallinity analysis

Crystallinity analysis was performed using a powder diffractometer (TD-3500, Dandong Tongda Science and Technology Co., Ltd, China). The powder pattern of samples was collected at a 2θ diffraction angle from 3° to 60° (step size 0.02° 2θ, time per step: 5 s) in reflection mode. The scanning speed was 5000°/min. The interplanar spacing was calculated using Bragg Equation: 2 d sinθ = n λ [22].

2.11. Simulated saliva-gastrointestinal digestion

Fresh saliva was collected from six healthy volunteers and centrifuged at −20 °C to simulate oral digestion. The gastric electrolyte solution (GES) and the small intestinal electrolyte solution (SIES) were obtained according to the reported methods (Table S2) [23]. The gastric medium contained 150 g of GES, 35.4 mg of pepsin and 37.5 mg of gastric lipase, and the final pH was adjusted to 2 using HCl (0.1 M). The small intestinal medium (120 g) was composed of SIES, 4% bile salt liquor (w/w) and 7% bile salt solution(w/w) at a mass ratio of 1: 2: 1 with 3.9 mg of trypsin, and the pH was adjusted to 7 by the addition of $NaHCO_3$(1 M). The saliva and the sample solution (5 mg/mL) were fully mixed in equal volumes and maintained at 37 °C for 3 min. Salivary digestion residual liquid (10 mL) was mixed with simulated gastric fluid (10 mL). Thereafter, the pH was adjusted to 3.0. The mixtures were then incubated at 37 °C for 2 h. Subsequently, the simulated small intestinal fluid (3 mL) with digested simulated gastric solution (10 mL) were mixed. Next, the pH was adjusted to 7.0. Afterward, the mixture was incubated at 37 °C for 2 h. The distilled water was added to the simulated digestion medium as the blank control group. Each experiment was repeated in triplicate.

2.12. Measurement of Mw change and chemical properties

The reducing sugar content of digestion products was determined by the dinitrosalicylic acid (DNS) method [24]. The free monosaccharides of samples were investigated by using an HPLC system equipped with an ELSD. The column and elution gradients used were shown in Supplementary Materials Table S3 and Table S4, respectively. The Mw and total sugar were measured as described previously.

2.13. Fermentation in vitro of FVPs

The fermentation medium was prepared according to the method of Zhang et al. [25]. The fresh fecal samples were provided by four healthy volunteers (two males and two females) who kept on a regular diet without antibiotic or probiotic treatment for at least 3 months. Equal amounts of feces taken from each volunteer were mixed with sterile modified saline (cysteine-HCl 0.5 g/L, NaCl 9 g/L) to afford feces suspension (10%, w/v). The fecal suspension was centrifuged at 500 × g for 5 min, and the supernatant was immediately kept in the anaerobic environment for use. Then, 1 mL of fecal suspension and 9 mL of basal medium with 100 mg sample were mixed in a sterilized centrifuge tube. The basal nutrient medium (the blank group) and the basal nutrient medium with 100 mg of inulin (the inulin group) were set as the negative and positive control under the same conditions, respectively. The fermented samples were collected at 0, 6, 12, 24, and 48 h for further analysis. The initial microbial community was recorded as OR group. All fermentation experiments were repeated five times.

2.14. Analysis of pH, SCFAs and lactic acid

The contents of SCFAs were measured by gas chromatography (GC) [26]. GC was performed using an HP-Innowax capillary column (30 m × 0.25 mm × 0.25 μm, J & W Scientific, Agilent) and flame ionization detector (FID). The conditions for GC analysis were shown in Supplementary Materials Table S5. The content of lactic acid was estimated with an HPLC system equipped with a UV–Vis detector at 210 nm [27]. The liquid chromatographic condition was shown in Supplementary Materials Table S6. A micro-pH meter (PHS-3C, China) was used to determine the pH. Five replicate readings were done for each sample.

2.15. Analysis of gut microbiota

The genomic DNA of the total bacteria was extracted by the TopTaq DNA Polymerase kit (Tiangen Biotech Co., Ltd., Beijing, China). The primers specific for the V3-V4 region of the 16 s rRNA gene were shown in Table S7. A specific index sequence was added and the PCR products were purified for library construction. High-throughput sequencing was performed on the Illumina MiSeq platform to generate 2 × 250 bp paired-end reads after the library was quantified, pooled and quality checked [28].

2.16. Ethical approval

Volunteers were mentally and physically able to participate in the study and informed written consent was obtained from each volunteer. All experiments were performed in compliance with the relevant laws and institutional guidelines.

2.17. Statistical analysis

All experiments were performed at least three times. Analysis of variance (ANOVA) and Spearman correlation analysis were performed using SPSS-22 software (SPSS Inc., Chicago, United States). Duncan test was used for significant difference analyses considering a 5% probability value. Principal component analysis (PCA) was carried out using SIMCA-14.1 software (Sartorius, Gottingen, Germany).

3. Results and discussion

3.1. Degradation kinetics of FVP

3.1.1. Degradation kinetics of FVP under different ultrasonic intensities

Under the same ultrasonic intensity, the Mw of FVP decreased fast followed by slow with treatment time (Fig. 1a). This was probably because that the degradation and fracture of polymer in solution were mainly caused by friction between solvent and polymer chain during the collapse of cavitation bubbles. The effect only worked on some larger polymer chains. The number of small polymer chains of FVP increased with treatment time, so the degradation rate of FVP slowed down [29]. Furthermore, the reduction in Mw was higher at a high ultrasonic intensity at the same treatment time. The degradation process of FVP at different ultrasonic intensities was fitted by the 0 order, 1st order and 2nd order kinetics models, and the reaction rate constants and correlation coefficients were shown in Table 2. According to the correlation coefficient (R^2), the 2nd order mathematical model was the most workable to describe the degradation kinetics of FVP. The kinetic curves of FVP at different ultrasonic intensities were shown in Fig. 1a. When the ultrasonic intensity increased from 531 W/cm^2 to 3185 W/cm^2, the reaction rate constant k_2 increased significantly from 1.829×10^{-4} to 6.131×10^{-4}. With the increase of ultrasonic intensity, the degradation rate of polysaccharides increased rapidly at first and then slowly. The results could be explained that higher ultrasonic intensity could increase the mechanical bond-breaking effect, leading to the degradation of more macromolecular polysaccharides under the effect of high-speed vibration and shear force. Furthermore, the cavitation effect and the number of cavitation bubbles increased with the increase of ultrasonic intensity [30].
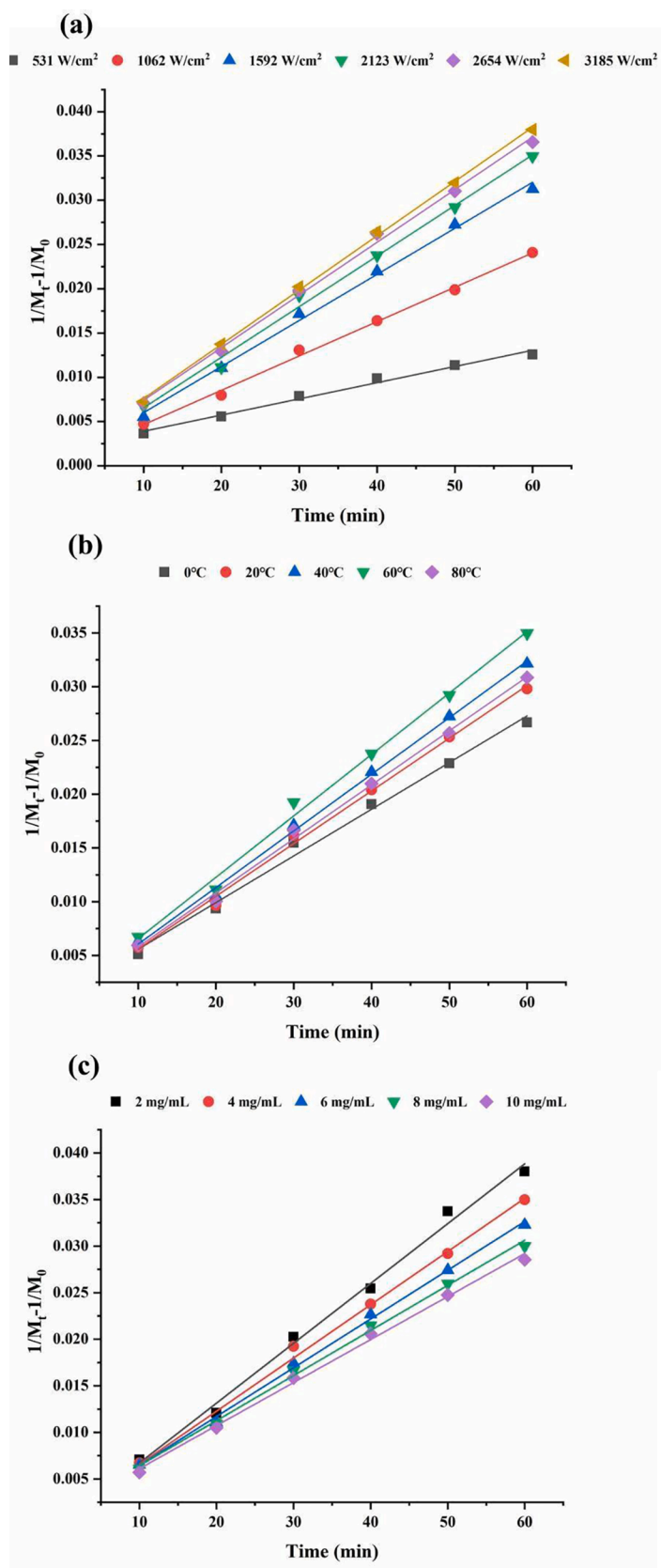
Fig. 1. The kinetic curve of FVP degradation at different ultrasonic intensities (a), ultrasonic temperatures (b) and concentrations (c).

Table 2
Constant parameters of molecular weight equation for FVP solution under different ultrasound intensities.

Ultrasonic intensities (W/cm^2)	0 order		1st order		2nd order	
	k_0	R^2	k_1 (min^{-1})	R^2	k_2 (mol·g^{-1}·min^{-1})	R^2
531	0.324	0.961	0.767×10^{-2}	0.977	1.829×10^{-4}	0.988
1062	0.466	0.958	1.325×10^{-2}	0.986	3.882×10^{-4}	0.997
1592	0.496	0.926	1.572×10^{-2}	0.973	5.205×10^{-4}	0.996
2123	0.488	0.938	1.623×10^{-2}	0.977	5.714×10^{-4}	0.995
2654	0.478	0.931	1.656×10^{-2}	0.975	6.019×10^{-4}	0.997
3185	0.475	0.929	1.665×10^{-2}	0.978	6.131×10^{-4}	0.999

3.1.2. Degradation kinetics of FVP at different ultrasonic temperatures

The effect of temperature on the ultrasonic degradation of FVP is that the degradation rate increased with the ultrasonic water bath temperature increased from 0 °C to 60 °C. However, when the ultrasonic water bath temperature increased further (from 60 °C to 80 °C), the degradation rate of FVP decreased. The 2nd order kinetics model had the largest R^2 (Table 3), so it was most suitable for describing the ultrasonic degradation process of FVP at different temperatures. Fig. 1b presented the kinetic curves of FVP at different temperatures. Compared with the treatment group at 0 °C, the reaction rate constant k_2 of the treatment group at 60 °C was increased from 4.342×10^{-4} to 5.715×10^{-4}. But the reaction rate constant was decreased to 5.026×10^{-4} when the temperature increased to 80 °C. This result could be caused by the combined action of ultrasonic cavitation and the thermal effect. The increase of temperature intensified the molecular thermal movement, thus promoting the degradation of FVP [31]. Particularly, the degradation rate reached the maximum at 60 °C. As the temperature continues to increase, the high temperature of the liquid led to the high vapor pressure in bubbles, which enhanced the buffering effect when bubbles closed, and then weakened the cavitation effect [32].

3.1.3. Degradation kinetics of FVP with different concentrations

The FVP solutions with the concentration of 2, 4, 6, 8 and 10 mg/mL were prepared to assess the effect of concentration on FVP degradation (Table 1). After ultrasound treatment for 60 min, the Mw of FVP with different solution concentrations ranged from 18.57 kDa to 22.52 kDa. The Mw of FVP decreased more at lower concentrations. In order to obtain the reaction rate constant and express the relationship between polysaccharide concentration and the degradation rate of FVP. The data were further analyzed dynamically (Table 4). The 2nd order kinetics model well fit the degradation kinetic curves of FVP at different concentrations, and their correlation coefficients (R^2) were not less than 0.994. Fig. 1c presented the kinetic curves of FVP at different concentrations. The maximum reaction rate constant k_2 was 6.423×10^{-4} when the concentration was 2 mg/mL. With the increase of concentration, the reaction rate constant gradually decreased to 4.618×10^{-4}. This could be attributed to the greater possibility of depolymerization and glycosidic bond breakage caused by effective shearing of the polymer chain in

dilute solution [33]. With the decrease of concentration, the winding connection between chains became less intense [34]. In a thinner solution, the random coil structure of polysaccharides extended freely. Therefore, the polysaccharide chain was not entangled and the cavitation bubbles became larger [35]. The velocity gradient around collapsed bubbles was larger at a lower concentration, which was beneficial to ultrasonic degradation.

According to the ultrasonic degradation kinetics of FVP, three kinds of FVPs with high, medium and low Mw were selected for further study, including the original polysaccharide (FVP) and its ultrasonic degradation products (U-FVPs). U-FVPs were obtained when ultrasonic intensities equal to 531 (U-FVP1) and 3185 W/cm^2 (U-FVP2) were applied to 4 mg/mL FVP solution at 60 °C for 60 min.

3.2. Effects of ultrasonic modification on the physicochemical properties of FVP

3.2.1. Chemical components, particle size and ζ-potential

Compared with FVP, the particle size of U-FVP1 and U-FVP2 were decreased after ultrasonic degradation (Table 5). The result was consistent with the Mw change trend. However, the absolute value of ζ-potential of FVP increased after ultrasonic degradation (Table 5). The hydrodynamic size and charges of polysaccharides could indicate the stability of solution or colloid [36]. The larger negative charge and smaller particle size indicated that U-FVP1 and U-FVP2 had good solution stability. In addition, there was no significant difference in the total sugar content and protein content of FVP after ultrasonic treatment. However, the uronic acid content was increased, which might be due to the exposure of more uronic acid located inside the polysaccharide by ultrasonic treatment.

3.2.2. Conformation analysis

The results of the I_2-KI test were depicted in Fig. 2a. The maximum absorption peaks of FVP, U-FVP1 and U-FVP2 were basically concentrated on 353 nm while there were no peaks observed around 565 nm, indicating that there were many branches attached to the backbones of FVP, U-FVP1 and U-FVP2. Ultrasonic treatment did not change the complex branch structure of FVP [37].

Fig. 2b showed that the λ_{max} of complexes formed by FVP, U-FVP1 and U-FVP2 had a red shift compared with Congo red, indicating that all three polysaccharides had triple-helical conformation. However, when the concentration of NaOH increased to 0.10 mol/L and 0.05 mol/L, the λ_{max} of U-FVP1 and U-FVP2 began to decrease. This phenomenon indicated that the helical structure of polysaccharide began to disintegrate into random coils and no longer formed a complex with Congo red. The results suggested that ultrasonic modification destroyed the stability of the triple helix structure of FVP. The length of the backbone chain, with or without branched-chain, and the Mw will affect the stability of the triple helix chain [38].

The circular dichroism of polysaccharides was related to their molecular structure and conformation. As shown in Fig. 2c, FVP and U-FVPs showed a negative Cotton effect. After ultrasonic modification, the minimum absorption of FVP decreased and had a slight blue shift. The shift of the minimum absorption might be attributed to the n → π* transition of the carboxyl group and intramolecular and intermolecular

Table 3
Constant parameters of molecular weight equation for FVP solution at different ultrasound temperatures.

Ultrasonic temperatures (°C)	0 order		1st order		2nd order	
	k_0	R^2	k_1 (min^{-1})	R^2	k_2 (mol·g^{-1}·min^{-1})	R^2
0	0.473	0.930	1.409×10^{-2}	0.969	4.342×10^{-4}	0.992
20	0.486	0.948	1.515×10^{-2}	0.990	4.903×10^{-4}	0.997
40	0.485	0.950	1.565×10^{-2}	0.992	5.268×10^{-4}	0.998
60	0.488	0.938	1.633×10^{-2}	0.989	5.715×10^{-4}	0.995
80	0.485	0.947	1.530×10^{-2}	0.991	5.026×10^{-4}	0.997

Table 4
Constant parameters of molecular weight equation for FVP solution with different concentrations.

Concentration of polysaccharide (mg/mL)	0 order		1st order		2nd order	
	k_0	R^2	k_1 (min^{-1})	R^2	k_2 (mol·g^{-1}·min^{-1})	R^2
2	0.501	0.940	1.749×10^{-2}	0.979	6.423×10^{-4}	0.994
4	0.488	0.938	1.633×10^{-2}	0.977	5.715×10^{-4}	0.995
6	0.474	0.945	1.544×10^{-2}	0.982	5.235×10^{-4}	0.998
8	0.465	0.938	1.473×10^{-2}	0.977	4.841×10^{-4}	0.997
10	0.466	0.937	1.441×10^{-2}	0.976	4.618×10^{-4}	0.996

Table 5
Physicochemical properties of FVP, U-FVP1 and U-FVP2.

Physicochemical properties	Samples		
	FVP	U-FVP1	U-FVP2
M_w (kDa)	63.02 ± 0.11^a	35.18 ± 0.13^b	18.56 ± 0.09^c
Particle size (nm)	296.7 ± 7.75^a	157.6 ± 6.30^b	60.59 ± 9.34^c
ζ-potential (mv)	-10.13 ± 0.40^a	-15.70 ± 0.60^b	-21.06 ± 0.87^c
Total sugar content (%)	94.52 ± 0.007^a	94.46 ± 0.006^a	94.40 ± 0.009^a
Protein content (%)	1.73 ± 0.042^a	1.66 ± 0.062^a	1.75 ± 0.031^a
Uronic acid content (%)	2.319 ± 0.065^c	2.848 ± 0.057^b	3.351 ± 0.124^a

Value is expressed as mean $\pm$ SD (n = 3), means with different letters within the same factors are significantly different ($P < 0.05$)

interactions affecting the optical activity of carboxyl chromophores [39]. The change of negative ellipticity indicated the increase of molecular asymmetry [40]. This was mainly because the degradation of FVP exposed more carboxyl groups inducing the changes of the microenvironment around the carboxyl sites [41]. The effects of calcium ion and Congo red stain on the Circular dichroism curves of FVP, U-FVP1 and U-FVP2 were seen in Fig. 2d-f. Ca^{2+} did not enhance the negative Cotton effect of FVP, suggesting that there was no coordination binding between FVP and Ca^{2+}. After adding calcium ion, the negative Cotton effect of U-FVP1 and U-FVP2 were enhanced in different degrees, indicating that the binding ability between FVP and calcium ion was enhanced after ultrasonic modification. The negative Cotton effect of the three polysaccharides was enhanced after adding Congo red staining agent, indicating that they all had a triple helix structure, which was consistent with the results of the Congo red staining experiment. In conclusion, ultrasonic modification changed the structure and chain conformation of FVP, and this change increased with the increase of ultrasonic intensity.

3.2.3. Rheological properties analysis

Fig. 3a showed the effect of ultrasonic degradation on the apparent viscosity of FVP solution. The results showed that FVP and U-FVPs solutions were pseudoplastic fluids due to the typical shear dilution behavior that appeared in their apparent viscosity. The apparent viscosities of FVPs solutions decreased with the increase of degradation intensity. The result demonstrated that ultrasound could effectively reduce the apparent viscosities of FVP solution. As the increase of ultrasonic intensity, the dependence of shear rate on apparent viscosity was decreased gradually. Meanwhile, the shear-thinning was weakened. The effects of ultrasound on the storage modulus (G') and loss modulus (G'') of FVP were investigated (Fig. 3b). G' and G'' are the ratio of elastic stress to strain and the ratio of viscous stress to strain, respectively. The G' was higher than G'' of FVP, which indicated that FVP solution could be seen as a typical weak gel due to its solid-like behavior. Both G'' and G' of FVP increased with frequency. After ultrasonic modification, there was a decrease in the G' and G'' of FVP, and the G'' decreased faster, leading to the significant increase in tanδ (ratio of G'' to G'). In addition, the frequency dependence of the two moduli decreased. The results indicated that ultrasound changed the gel properties of FVP. The G'' and G' of U-FVP2 decreased to close to 0. The crossover frequency between viscous and elastic behavior of U-FVP2 was around 85 rad/s, indicating

the existence of transition viscoelasticity [42]. Therefore, ultrasound modification reduced the elasticity of FVP solution and increased the viscidity at a higher frequency. The decrease of elasticity of FVP might be related to the decrease of its Mw.

3.2.4. Crystallinity analysis

XRD helps analyze the microstructure of crystalline materials. XRD patterns were shown in Fig. 3c. The peaks of the X-ray diffraction intensity curves of FVP, U-FVP1 and U-FVP2 emerged at approximately 18.44°, 18.54° and 18.62°, respectively. The peaks' shapes were similar and round, which was the characteristic of a typical steamed bread peak. This was a typical diffraction pattern of high molecular polymer, indicating a low crystallinity [43]. The large width of the peak indicated the existence of a variety of similar crystal morphology and lattice types in the crystalline part. The interplanar spacing of the three polysaccharides were 3.79, 5.00 and 6.73 Å, respectively. Both FVP and U-FVPs could form crystals, but the crystal constants of U-FVPs were slightly larger than that of FVP. The crystal constants of U-FVP2 with the smallest Mw were the largest. It's about twice that of FVP. The results indicated that ultrasonic modification improved the crystallinity of FVP.

3.2.5. Thermal stability analysis

Fig. 3d showed the DSC curves of FVP, U-FVP1 and U-FVP2 under the protection of nitrogen. There were two endothermic stages in the heating process of the samples. The first stage was between 60 and 100 °C, which was connected with the evaporation of adsorbed water. The second stage was to absorb heat for oxidative decomposition [44]. The main change parameters of the second stage were shown in Table 6. Compared with FVP, the temperature at the onset of degradation (T$_O$) and enthalpy change (ΔH) of the U-FVPs were increased. The thermal stability of different polysaccharides was as follows: U-FVP2 > U-FVP1 > FVP. Ultrasonic degradation improved the thermal stability of FVP, and the increase of ultrasonic intensity contributed to the improvement of thermal stability. The improvement of thermal stability might be due to the decrease of the Mw and the increase of the crystallinity.

3.3. Effects of ultrasonic modification on the prebiotic activity

3.3.1. Characterization of FVPs during simulated digestion in vitro

Mw changes of FVP and U-FVPs in saliva, simulated gastric juice and pancreatic juice were shown in Table 7. The salivary amylase activity collected in this experiment was 175 ± 5 D units/mL, which was classified as normal as the data (20–250 D units/mL) [45]. After digestion by saliva, gastric juice and pancreatic juice, the average Mw of three FVPs did not change significantly ($P > 0.05$). As shown in Fig. S1-2, the contents of reducing sugar and total sugar did not change after digestion by saliva, simulated gastric juice and pancreatic juice ($P > 0.05$), which was consistent with the result of Mw determination. The results showed that both FVP and U-FVPs had anti-digestibility.

3.3.2. Characterization of FVPs during fermentation in vitro

3.3.2.1. Change of pH value during fermentation. The shift of the pH during fermentation was analyzed (Table S8). The initial pH of the inulin group and experimental groups was slightly lower than that of the blank
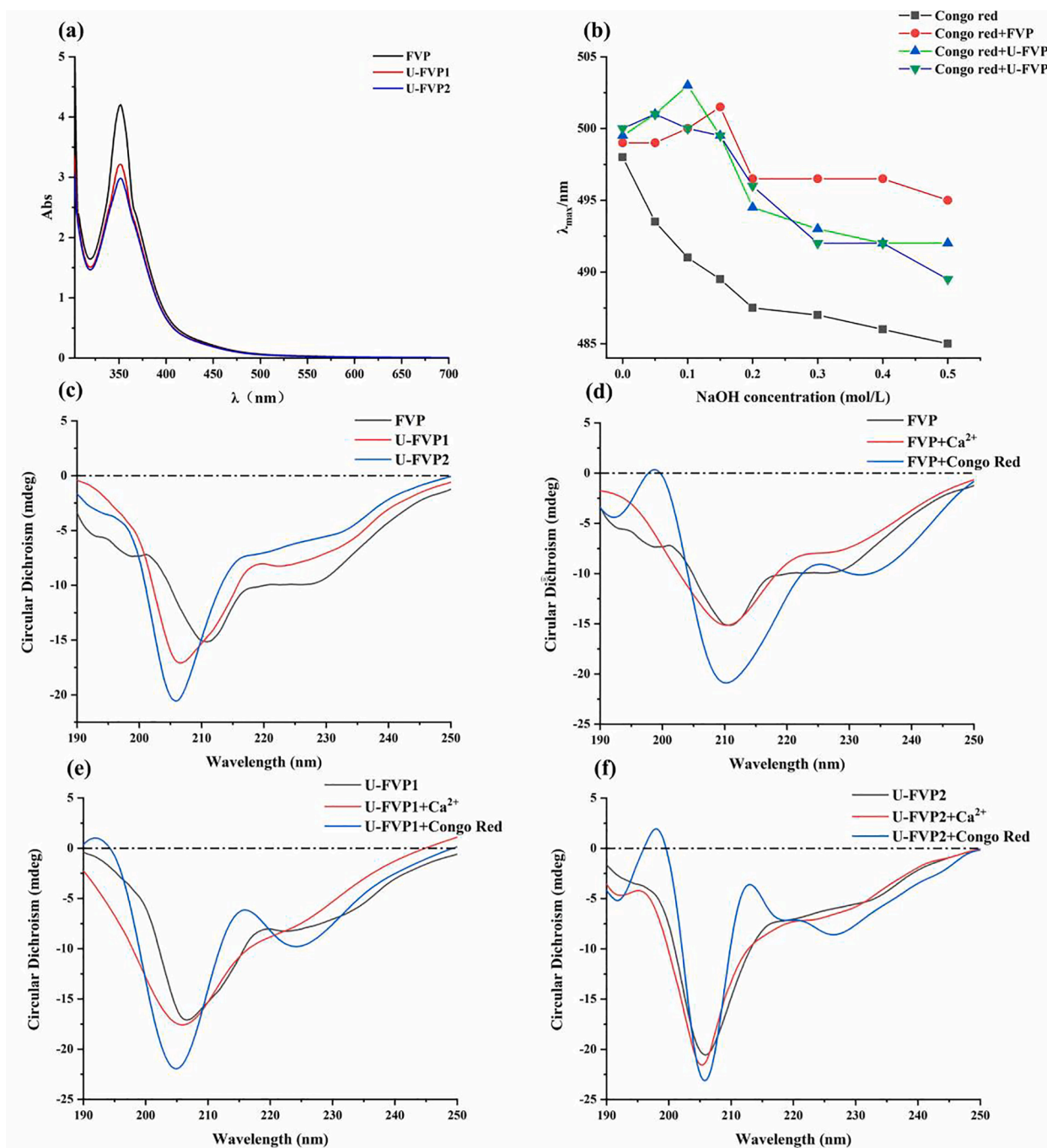
Fig. 2. Ultraviolet–visible absorption spectra of FVP, U-FVP1 and U-FVP2 reaction with I_2-KI (a); Maximum absorption wavelength of Congo red and Congo red with FVPs at various concentrations of NaOH (b); CD curve of FVP and its ultrasonic modified fractions (c); The effects of calcium ion and Congo red on the CD curve of FVP (d), U-FVP1 (e) and U-FVP2 (f). (For interpretation of the references to colour in this figure legend, the reader is referred to the web version of this article.)

group. The observed results could be devoted to the fact that the aqueous solutions of FVP and inulin were faintly acidic [46,47]. After fermentation, the pH of blank, FVP, U-FVP1, U-FVP2 and inulin group were 7.60 ± 0.01, 4.34 ± 0.01, 4.40 ± 0.01, 4.25 ± 0.01 and 4.24 ± 0.01, respectively. The pH of U-FVP2 was significantly lower than that of FVP and U-FVP1 group ($P < 0.05$), and there was no significant difference between U-FVP2 and inulin groups ($P > 0.05$). It has been reported that the complex metabolism of microorganisms could affect the pH of the intestine, which was mainly related to the production of some short-chain fatty acids [48].

3.3.2.2. SCFA production during fermentation. Fig. 4 showed the types

and concentration of SCFAs at 0, 6, 12, 24 and 48 h of fermentation. Through fermentation, the concentration of total SCFAs in U-FVP2 group was increased from 1.47 ± 0.13 to 84.49 ± 2.38 mM (Fig. 4a). The content of total SCFAs in U-FVP2 group was significantly higher than that in FVP and U-FVP1 group. There was no significant difference in the content of SCFAs between FVP group and U-FVP1 group ($P > 0.05$). Acetic acid, propionic acid and *n*-butyric acid were the main SCFAs increasing during the process of fermentation. Acetic acid and propionic acid were the energy sources of surrounding tissues [49]. They were also anti-inflammatory modulators and vasodilators, which could promote intestinal motility and trauma recovery [50]. Butyric acid, an energy source for colon epithelial cells, could regulate the growth and apoptosis
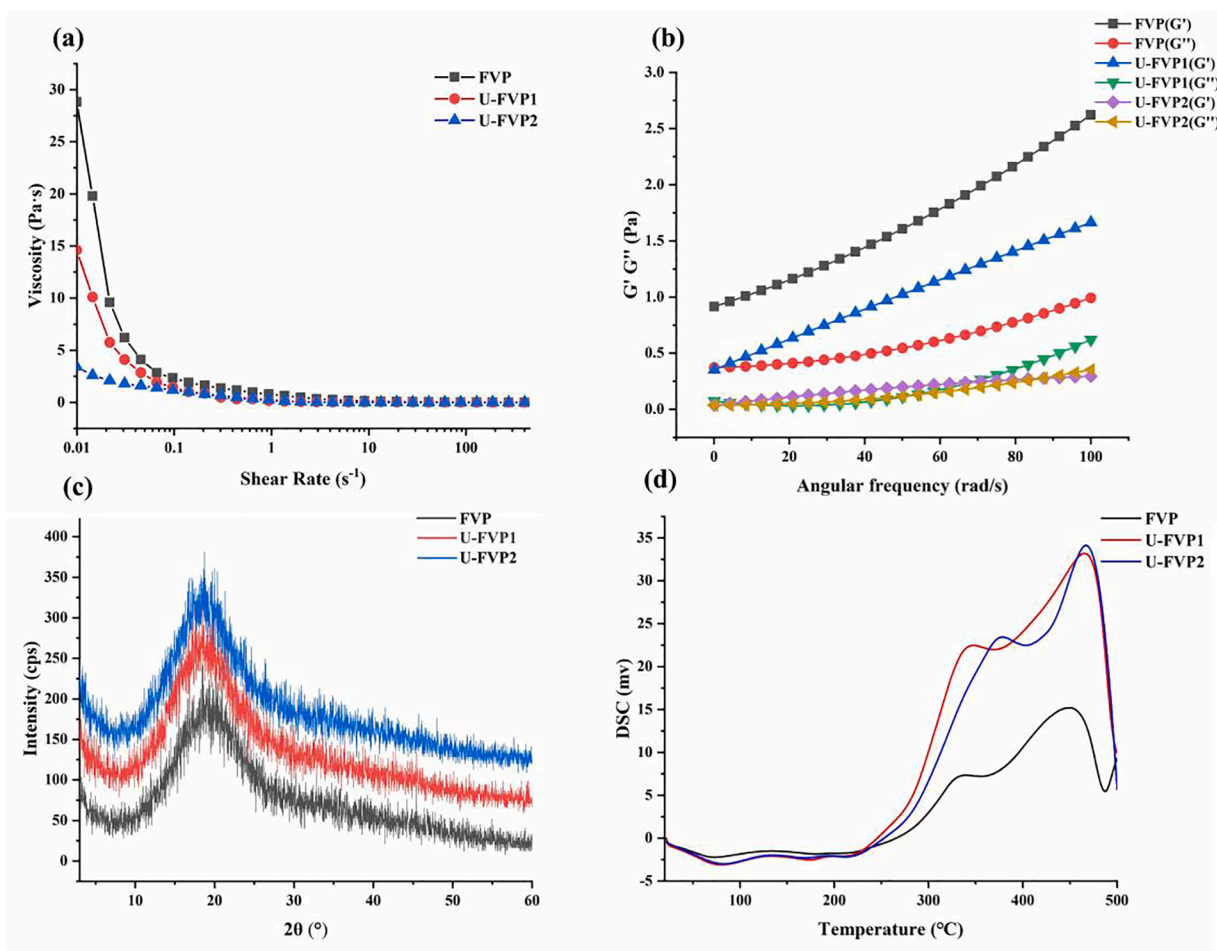
Fig. 3. Effect of ultrasonic depolymerization on the apparent viscosity of FVP (a); Effects of ultrasonic depolymerization on the elastic modulus (G′) and viscous modulus (G″) of FVP (b); The XRD intensity curves of FVP, U-FVP1 and U-FVP2 (c); The DSC curves of FVP, U-FVP1 and U-FVP2 (d).

Table 6
The DSC parameters of FVP, U-FVP1 and U-FVP2.

Samples	T_O[a] (°C)	T_T[b] (°C)	T_p[c] (°C)	ΔH[d] (J/g)
FVP	333.98	383.00	355.10	73.28
U-FVP1	347.80	426.42	369.32	157.58
U-FVP2	380.93	449.83	396.60	298.37

[a] T_O: onset temperature.
[b] T_T: termina temperature.
[c] T_P: peak temperature.
[d] ΔH: enthalpy change.

Table 7
Variations of MWs of FVPs after simulated oral, gastric and small intestinal digestion.

	M_W (kDa) Time (min)	FVP	U-FVP1	U-FVP2
Oral	0	63.05 ± 0.11^a	35.14 ± 0.13^a	18.57 ± 0.17^a
	2	63.13 ± 0.08^a	35.11 ± 0.12^a	18.60 ± 0.06^a
Gastric	0	63.07 ± 0.14^a	35.17 ± 0.11^a	18.62 ± 0.14^a
	30	62.98 ± 0.18^a	35.13 ± 0.09^a	18.59 ± 0.08^a
	60	63.10 ± 0.12^a	35.07 ± 0.08^a	18.61 ± 0.11^a
	90	63.07 ± 0.07^a	35.21 ± 0.08^a	18.56 ± 0.13^a
	120	63.01 ± 0.13^a	35.08 ± 0.17^a	18.53 ± 0.12^a
Intestinal	0	63.11 ± 0.16^a	35.13 ± 0.11^a	18.70 ± 0.12^a
	30	62.94 ± 0.09^a	35.24 ± 0.15^a	18.60 ± 0.08^a
	60	63.16 ± 0.16^a	35.11 ± 0.13^a	18.63 ± 0.14^a
	90	63.06 ± 0.06^a	35.07 ± 0.16^a	18.59 ± 0.05^a
	120	62.96 ± 0.15^a	35.01 ± 0.17^a	18.41 ± 0.11^a

Value is expressed as mean ± SD (n = 3), means with different letters within the same factors are significantly different ($P < 0.05$)

of epithelial cells and immune cells, inhibiting colitis and colon cancer [51]. U-FVP2 group showed the highest contents in acetic acid and propionic acid. However, FVP group showed the highest content in *n*-butyric acid. During the period from 24 h to 48 h, the content of *n*-butyric acid decreased in U-FVPs groups and inulin group. This might be due to the fact that nutrients in the medium could no longer meet the growth and reproduction of gut microbiota, resulting in the decomposition and utilization of *n*-butyric acid. The contents of *i*-butyric acid, *n*-valeric acid and *i*-valeric acid were low. Compared with the blank group, the content of *n*-valeric acid decreased in inulin and experimental groups, and that of inulin group and U-FVP2 group was the lowest. It was possibly due to that *n*-valeric acid was the product of protein fermented by spoilage bacteria, and the addition of polysaccharides inhibited this adverse fermentation [52]. In addition, lactic acid was also produced in inulin group during fermentation. As shown in Fig. 4h, the content of lactic acid in the inulin group was the highest after

fermentation for 6 h (7.81 ± 0.02 mm). As the initial product of fermentation, lactic acid could be used by some microorganisms to produce propionic acid, butyric acid and acetic acid [53].

3.3.2.3. Composition of intestinal microbiota. The alpha diversity, including the Shannon index and Simpson index of each group was represented in Fig. 5a-b. Compared with the blank group, the microbial community diversity in experimental groups decreased in different
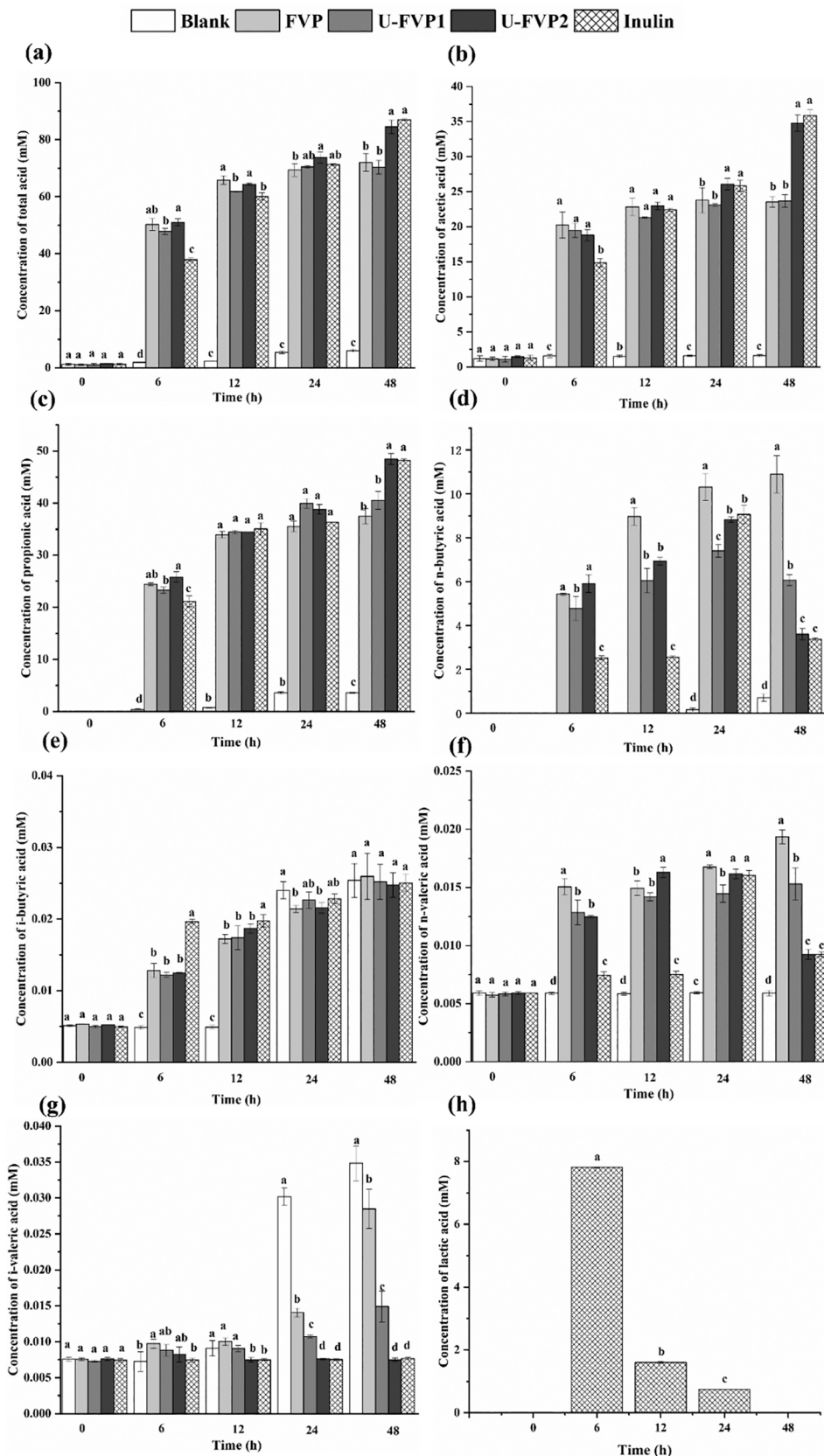
Fig. 4. Concentrations of total SCFAs (a), acetic acid (b), propionic acid (c), *n*-butyric acid (d), *i*-butyric acid (e), *n*-valeric acid (f) and *i*-valeric acid (g) in fermentation solutions at different time points during the *in vitro* fermentation; Concentrations of lactic acid in inulin group (h). The data are mean ± SD, n = 5 per group. Different lowercase letters mean significant difference (*P* < 0.05) in the contents at the same time point.
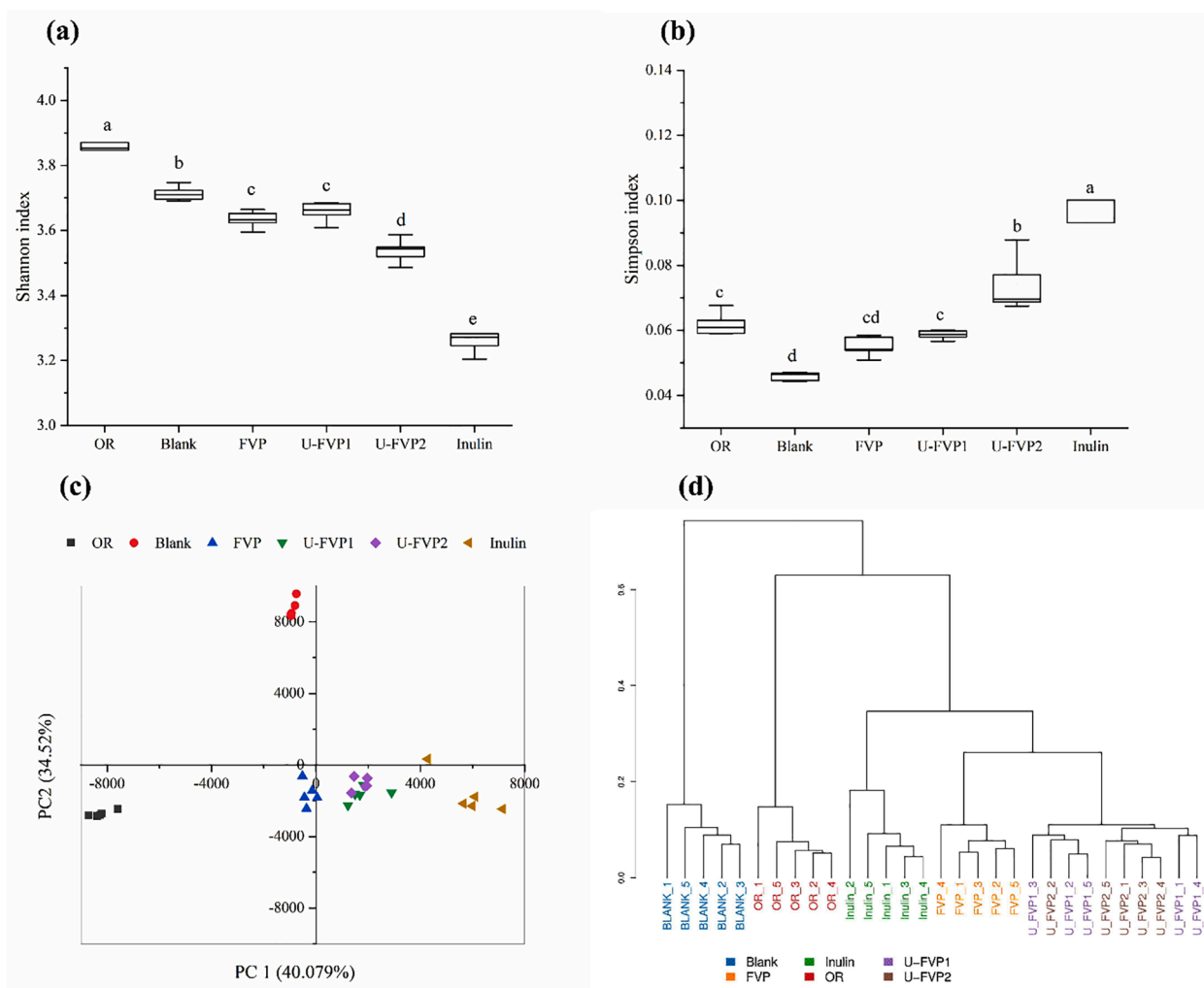
Fig. 5. Shannon index (a) and Simpson index (b) of the samples cultured *in vitro*; The PCA (c) and Cluster analysis (d) of overall bacterial composition between each group. Different lowercase letters mean significant difference ($P < 0.05$) of the diversity index in different groups.

degrees. The community diversity of U-FVP2 group was significantly lower than FVP and U-FVP1 group. The decrease of the richness in polysaccharide groups was mainly due to the rapid proliferation of some bacteria that could use polysaccharides, which inhibited the growth of other bacteria [5]. The principal component analysis (PCA) revealed the overall difference among different treatments with respect to microorganism composition. The treatment groups were significantly separated from the blank group in the PCoA score chart, suggesting that FVPs and inulin had great influence on the gut microbiota community. More importantly, the U-FVPs groups were different from the FVP group in the quadrant, but they were the same as the inulin group. This phenomenon indicated that the effects of U-FVPs on gut microbiota were different from FVP but similar to inulin. Moreover, a cluster trees map based on the Bray-Curtis method was used to analyze the similarity of groups (Fig. 5d). The shorter branch length represented the similar microbiota community of samples, which was following the result of the PCA analysis.

At the phylum level (Fig. 6a), the gut microbial before fermentation (OR) was mainly composed of *Firmicutes, Bacteroidetes, Proteobacteria* and *Actinobacteria*, especially *Firmicutes* and *Bacteroidetes,* accounting for 97.42%. It was highly consistent with the literature [54], indicating that the fecal samples used in this experiment were representative and feasible. After fermentation for 48 h, compared with the blank group, the relative abundance of *Bacteroidetes* was increased while *Firmicutes* was decreased in inulin group and experimental groups. The relative

abundance of *Bacteroidetes* in different groups was as follows: FVP > U-FVP1, U-FVP2 > inulin. *Firmicutes* and *Bacteroidetes* were closely related to the metabolism and energy absorption of the host intestinal flora [55]. The decrease in the ratio of *Firmicutes* to *Bacteroidetes* was connected with intestinal health [56]. Moreover, U-FVPs and inulin promoted the growth of *Actinobacteria*. However, the addition of polysaccharides inhibited the growth of *Proteobacteria*. The relative abundance of *Proteobacteria* in U-FVP1 group was the lowest, which was lower than that in inulin and FVP group. *Proteobacteria*, as a signature bacterium causing intestinal microecological imbalance and intestinal diseases, might increase the secretion of inflammatory factors, reduce human immunity and increase the risk of diseases [57]. Therefore, the regulation of FVP and U-FVPs on intestinal flora structure was beneficial to human health.

The analysis of specific bacteria at the genus level helps obtain more biological information (Fig. 6). Compared with blank group, both FVP and U-FVPS facilitated the growth of *Prevotella, Bacteroides, Faecalibacterium* and *Alloprevotella*, and inhibited the growth of harmful bacteria such as *Escherichia/Shigella, Clostridium_XlVa* and *Bilophila*. Although the abundance of *Prevotella* and *Bacteroides* in U-FVP1 and U-FVP2 group was lower than that in FVP group, U-FVPs had a significant growth-promoting effect on *Bifidobacterium* and *Blautia*. Early research found that individuals with *Prevotella*-dominated gut microbiota responded to barley kernel bread supplementation with improved glucose tolerance [58]. FVP is expected to be a functional food for
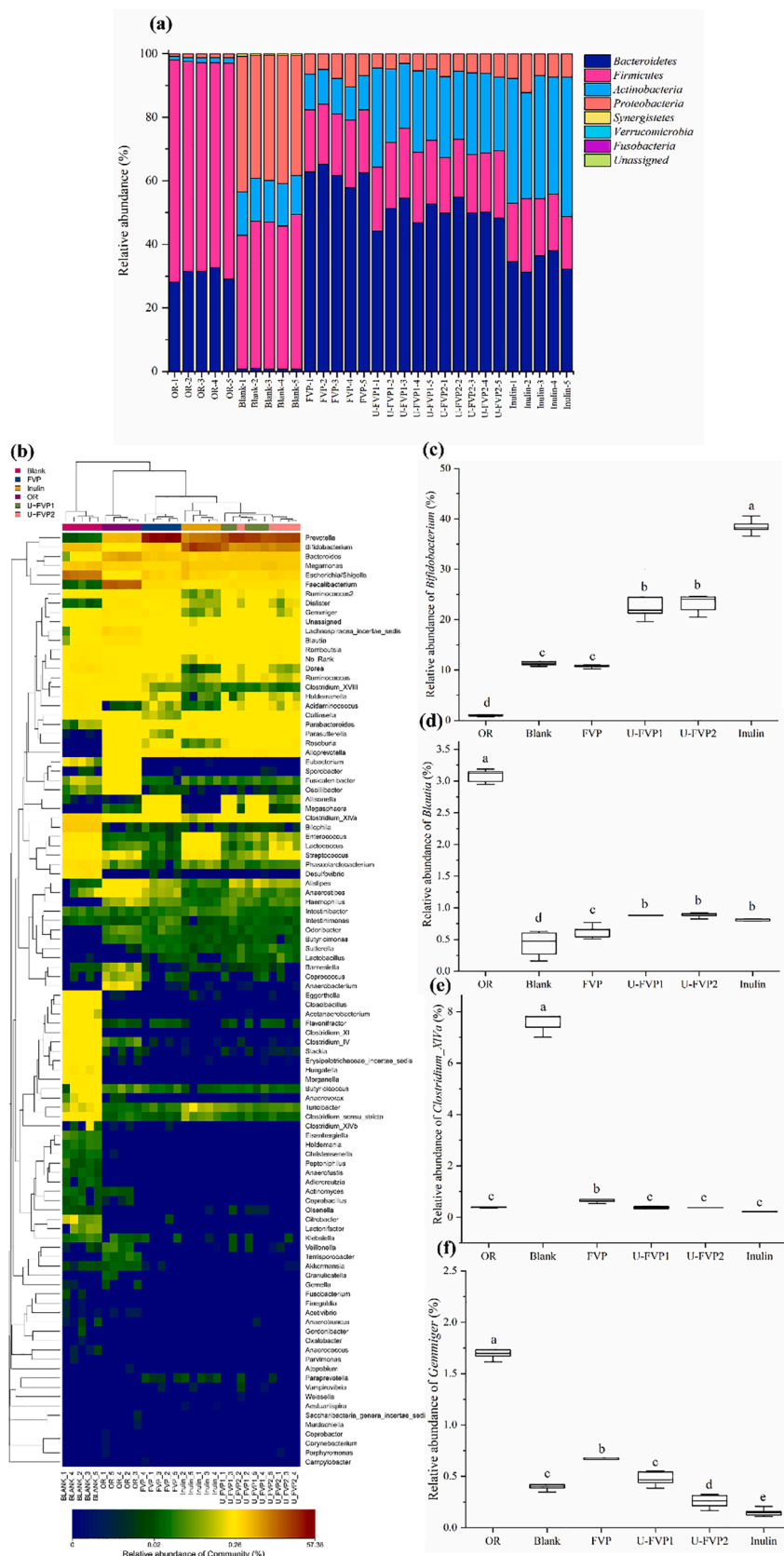
Fig. 6. Relative abundance of gut bacteria at the phylum level (a); Heatmap analysis of gut bacteria at the genus level (b); Relative abundance of *Bifidobacterium (c)*; Relative abundance of *Blautia (d)*; Relative abundance of *Clostridium_Xlva (e)*; Relative abundance of *Gemmiger (f)*. Different lowercase letters indicate a significant difference (*P* < 0.05) of the microbial relative abundance in different groups.

people with diabetes and obesity. *Bifidobacterium* was an important intestinal bacterium, which has many important physiological functions beneficial to human health, such as improving epithelial cell barrier function, enhancing intestinal immunity, antitumor effect and probiotic effects on gastrointestinal function [59]. Studies have found that the presence of *Blautia* could reduce the inflammatory levels and increase intestinal peristalsis [60,61]. In addition, *Blautia* has the ability to produce SCFAs in human intestinal fermentation, and it is mainly involved in the production of propionate and butyrate [62]. Besides, U-FVP1 and U-FVP2 had stronger inhibitory effects on *Escherichia/Shigella* and *Clostridium_XlVa*. Furthermore, U-FVP2 could also inhibit the growth of *Gemmiger*. It has been reported that the relative abundance *of Escherichia/Shigella* was positively associated with inflammation, intestinal barrier injuries and glucose metabolism disorders [63]. *Clostridium_XlVa* like *Clostridium difcile* is usually regarded as an opportunistic pathogen [64]. The relative abundance of *Gemmiger* has a significant positive effect on increased liver enzymes, ferritin and overweight [65]. These results demonstrated that U-FVPs, especially U-FVP2, could more effectively regulate the composition of intestinal flora by stimulating the growth of probiotics and inhibiting the growth of harmful bacteria, suggesting that U-FVPs had better prebiotic activity.

3.4. Correlation analysis

In order to study the relationship between the changes of physicochemical properties of FVP after ultrasonic modification and the gut microbiota, the correlation analysis was applied (Fig. S3). The abundance of *Prevotella* was found to exhibit a positive correlation with Mw, particle size, viscosity and thermal stability of FVPs. The Mw, particle size, ζ-potential of FVPs displayed negative associations with the abundance of *Bifidobacterium* and *Blautia*. However, the content of uronic acid and crystallinity showed positive associations with the abundance of *Bifidobacterium* and *Blautia*. The correlation between physicochemical properties and the abundance of the two harmful bacteria was completely opposite to probiotics. The abundance of *Clostridium_XlVa* and *Gemmiger* was positively correlated with Mw, particle size, potential and thermal stability, and negatively correlated with Glucuronic acid content and crystallinity. There was a close correlation between the Mw, Glucuronic acid content, particle size, ζ-potential, viscosity, crystallinity, thermal stability and gut microbiota. Interestingly, Mw showed a very high correlation with other physicochemical properties ($P < 0.01$) (Table S9). These phenomena indicated that the decrease of Mw might be an important factor for the change of other physicochemical properties of FVP by ultrasound. Previous study reported that Oligosaccharides have low Mw, less viscosity. These properties endow oligosaccharides with significant biological properties including the microbiota regulation ability [66]. Degradation products of polysaccharides with low Mw promoted the growth of beneficial bacteria in the intestine such as *bifidobacteria* and *Lactobacillus*, and effectively inhibit harmful microorganisms such as *Escherichia coli* [67,68]. Due to their better growth-promoting effect on *Prevotella*, polysaccharides with high Mw have the potential to prevent intestinal flora imbalance and obesity-related metabolic disorders in obese people [69].

4. Conclusion

In this study, the partial degradation of FVP by ultrasonic modification was investigated. Degradation kinetics analysis indicated the ultrasonic degradation of FVP fitted to the 2nd-order degradation kinetic model. Ultrasound intensity, temperature and polysaccharide concentration were the key factors in the degradation. The chain conformation changed when ultrasound was applied. The U-FVPs showed lower viscosity and gel strength, higher thermal stability. More importantly, The U-FVPs were more readily utilized by gut microbiota. After fermentation *in vitro*, U-FVPs could more effectively regulate the intestinal

microecology by producing more short-chain fatty acids, reducing intestinal pH value, promoting the growth of beneficial bacteria such as *Bifidobacterium* and *Brautella*, and inhibiting harmful bacteria. In conclusion, the results confirmed that ultrasound was a controllable method for partial degradation of FVP to improve its physicochemical and bioactive properties.

CRediT authorship contribution statement

Jinrong Xiao: Investigation, Writing – original draft, Writing – review & editing. **Xin Chen:** Validation, Formal analysis. **Qiping Zhan:** Writing – review & editing. **Lei Zhong:** Writing – review & editing. **Qiuhui Hu:** Supervision, Writing – review & editing. **Liyan Zhao:** Supervision, Writing – review & editing.

Declaration of Competing Interest

The authors declare that they have no known competing financial interests or personal relationships that could have appeared to influence the work reported in this paper.

Acknowledgements

Appendix A. Supplementary data

Supplementary data to this article can be found online at https://doi.org/10.1016/j.ultsonch.2021.105901.

References

[1] P.u. Jing, S.-J. Zhao, M.-M. Lu, Z. Cai, J. Pang, L.-H. Song, Multiple-fingerprint analysis for investigating quality control of Flammulina velutipes fruiting body polysaccharides, J. Agric. Food Chem. 62 (50) (2014) 12128–12133.

[2] M. Fukushima, T. Ohashi, Y. Fujiwara, K. Sonoyama, M. Nakano, Cholesterol-lowering effects of maitake (Grifola frondosa) fiber, shiitake (Lentinus edodes) fiber, and enokitake (Flammulina velutipes) fiber in rats, Exp. Biol. Med. 226 (8) (2001) 758–765.

[3] R. Zhao, Q. Hu, G. Ma, A. Su, M. Xie, X. Li, G. Chen, L. Zhao, Effects of Flammulina velutipes polysaccharide on immune response and intestinal microbiota in mice, J. Funct. Food. 56 (2019) 255–264.

[4] A. Su, W. Yang, L. Zhao, F. Pei, B. Yuan, L. Zhong, G. Ma, Q. Hu, Flammulina velutipes polysaccharides improve scopolamine-induced learning and memory impairment in mice by modulating gut microbiota composition, Food Funct. 9 (3) (2018) 1424–1432.

[5] A. Su, G. Ma, M. Xie, J. Yang, X. Li, L. Zhao, Q. Hu, Characteristic of polysaccharides from Flammulina velutipes invitro digestion under salivary, simulated gastric and small intestinal conditions and fermentation by human gut microbiota, Int. J. Food Sci. Technol. 54 (2019) 2277–2287.

[6] T. Requena, M.C. Martínez-Cuesta, C. Peláez, Diet and microbiota linked in health and disease, Food Funct. 9 (2) (2018) 688–704.

[7] J.L. Hu, S.P. Nie, C. Li, S. Wang, M.Y. Xie, Ultrasonic irradiation induces degradation and improves prebiotic properties of polysaccharide from seeds of Plantago asiatica L. during in vitro fermentation by human fecal microbiota, Food Hydrocolloids 76 (2018) 60–66.

[8] H. El Knidri, R. Belaabed, A. Addaou, A. Laajeb, A. Lahsini, Extraction, chemical modification and characterization of chitin and chitosan, Int. J. Biol. Macromol. 120 (2018) 1181–1189.

[9] M.J. Spotti, O.H. Campanella, Functional modifications by physical treatments of dietary fibers used in food formulations, Curr. Opin. Food Sci. 15 (2017) 70–78.

[10] M. Ma, T. Mu, Modification of deoiled cumin dietary fiber with laccase and cellulase under high hydrostatic pressure, Carbohydr. Polym. 136 (2016) 87–94.

[11] H.M. Saleh, M.S.M. Annuar, K. Simarani, Ultrasound degradation of xanthan polymer in aqueous solution: Its scission mechanism and the effect of NaCl incorporation, Ultrason. Sonochem. 39 (2017) 250–261.

[12] J. Gao, T. Zhang, Z.-Y. Jin, X.-M. Xu, J.-H. Wang, X.-Q. Zha, H.-Q. Chen, Structural characterisation, physicochemical properties and antioxidant activity of polysaccharide from Lilium lancifolium Thunb, Food Chem. 169 (2015) 430–438.

[13] Y. Xu, Y. Guo, S. Duan, H. Wei, Y. Liu, L. Wang, X. Huo, Y.u. Yang, Effects of ultrasound irradiation on the characterization and bioactivities of the polysaccharide from blackcurrant fruits, Ultrason. Sonochem. 49 (2018) 206–214.

[14] L. Zhang, X. Ye, T. Ding, X. Sun, Y. Xu, D. Liu, Ultrasound effects on the degradation kinetics, structure and rheological properties of apple pectin, Ultrason. Sonochem. 20 (1) (2013) 222–231.

[15] X. Chen, D. Fang, R. Zhao, J. Gao, B.M. Kimatu, Q. Hu, G. Chen, L. Zhao, Effects of ultrasound-assisted extraction on antioxidant activity and bidirectional immunomodulatory activity of Flammulina velutipes polysaccharide, Int. J. Biol. Macromol. 140 (2019) 505–514.

[16] H. Li, L. Pordesimo, J. Weiss, High intensity ultrasound-assisted extraction of oil from soybeans, Food Res. Int. 37 (7) (2004) 731–738.

[17] Y. Su, L. Li, Structural characterization and antioxidant activity of polysaccharide from four auriculariales, Carbohydr. Polym. 229 (2020), 115407.

[18] N. Blumenkrantz, G. Asboe-Hansen, New method for quantitative determination of uronic acids, Anal. Biochem. 54 (2) (1973) 484–489.

[19] Y. Ren, L. Jiang, W. Wang, Y. Xiao, S. Liu, Y.u. Luo, M. Shen, J. Xie, Effects of Mesona chinensis Benth polysaccharide on physicochemical and rheological properties of sweet potato starch and its interactions, Food Hydrocolloids 99 (2020) 105371, https://doi.org/10.1016/j.foodhyd.2019.105371.

[20] D. Šimková, J. Lachman, K. Hamouz, B. Vokál, Effect of cultivar, location and year on total starch, amylose, phosphorus content and starch grain size of high starch potato cultivars for food and industrial processing, Food Chem. 141 (4) (2013) 3872–3880.

[21] L.S.C. Kreisman J.H. Friedman A. Neaga B.A. Cobb Structure and function relations with a T-cell-activating polysaccharide antigen using circular dichroism 17 1 2007 2007 46 55.

[22] M. Poletto, H.L. Ornaghi Junior, A.J. Zattera, Native cellulose: Structure, characterization and thermal properties, Materials 7 (2014) 6105–6119.

[23] Y. Liu, Y. Li, Y.u. Ke, C. Li, Z. Zhang, Y. Wu, B. Hu, A. Liu, Q. Luo, W. Wu, In vitro saliva-gastrointestinal digestion and fecal fermentation of Oudemansiella radicata polysaccharides reveal its digestion profile and effect on the modulation of the gut microbiota, Carbohydr. Polym. 251 (2021) 117041, https://doi.org/10.1016/j.carbpol.2020.117041.

[24] L. Wang, C. Li, Q. Huang, X. Fu, R.H. Liu, In vitro digestibility and prebiotic potential of a novel polysaccharide from Rosa roxburghii Tratt fruit, J. Funct. Food. 52 (2019) 408–417.

[25] X. Zhang, J.J. Aweya, Z.-X. Huang, Z.-Y. Kang, Z.-H. Bai, K.-H. Li, X.-T. He, Y. Liu, X.-Q. Chen, K.-L. Cheong, In vitro fermentation of Gracilaria lemaneiformis sulfated polysaccharides and its agaro-oligosaccharides by human fecal inocula and its impact on microbiota, Carbohydr. Polym. 234 (2020) 115894, https://doi.org/10.1016/j.carbpol.2020.115894.

[26] R. Zhao, Y. Ji, X. Chen, A. Su, G. Ma, G. Chen, Q. Hu, L. Zhao, Effects of a beta-type glycosidic polysaccharide from Flammulina velutipes on anti-inflammation and gut microbiota modulation in colitis mice, Food Funct. 11 (2020) 4259–4274.

[27] Z. Zheng, S.T. Jiao, L.J. Pan, J. Huang, Study on determination of lactc acid content in fermentertion broth by RP-HPLC, Food Sci. (2003) 89–91 (in Chinese).

[28] M. Xie, G. Chen, P. Wan, Z. Dai, B. Hu, L. Chen, S. Ou, X. Zeng, Y.i. Sun, Modulating effects of dicaffeoylquinic acids from Ilex kudingcha on intestinal microecology in vitro, J. Agric. Food Chem. 65 (47) (2017) 10185–10196.

[29] X. Guo, X. Ye, Y. Sun, D. Wu, N. Wu, Y. Hu, S. Chen, Ultrasound effects on the degradation kinetics, structure, and antioxidant activity of sea cucumber fucoidan, J. Agric. Food Chem. 62 (5) (2014) 1088–1095.

[30] K. Houben, R.P. Jolie, I. Fraeye, A.M. Van Loey, M.E. Hendrickx, Comparative study of the cell wall composition of broccoli, carrot, and tomato: Structural characterization of the extractable pectins and hemicelluloses, Carbohydr. Res. 346 (2011) 1105–1111.

[31] H. Yang, J. Bai, C. Ma, L. Wang, X. Li, Y.u. Zhang, Y. Xu, Y.u. Yang, Degradation models, structure, rheological properties and protective effects on erythrocyte hemolysis of the polysaccharides from Ribes nigrum L, Int. J. Biol. Macromol. 165 (2020) 738–746.

[32] T. Mason, J. Lorimer, Applied sonochemistry: The uses of power ultrasound in chemistry and processing, Chem. Eng. Process. 9 (2003) 885–900.

[33] J.-K. Yan, J.-J. Pei, H.-L. Ma, Z.-B. Wang, Effects of ultrasound on molecular properties, structure, chain conformation and degradation kinetics of carboxylic curdlan, Carbohydr. Polym. 121 (2015) 64–70.

[34] Q. Zou, Y. Pu, Z. Han, N. Fu, S. Li, M. Liu, L. Huang, A. Lu, J. Mo, S. Chen, Ultrasonic degradation of aqueous dextran: Effect of initial molecular weight and concentration, Carbohydr. Polym. 90 (2012) 447–451.

[35] Y. Pu, Q. Zou, L. Liu, Z. Han, X. Wang, Q. Wang, S. Chen, Clinical dextran purified by fractional ultrafiltration coupled with water washing, Carbohydr. Polym. 87 (2) (2012) 1257–1260.

[36] G. Chen, X. Chen, B. Yang, Q. Yu, X. Wei, Y. Ding, J. Kan, New insight into bamboo shoot (Chimonobambusa quadrangularis) polysaccharides: Impact of extraction processes on its prebiotic activity, Food Hydrocolloids 95 (2019) 367–377.

[37] M. Sun, Y. Li, T. Wang, Y. Sun, X. Xu, Z. Zhang, Isolation, fine structure and morphology studies of galactomannan from endosperm of Gleditsia japonica var. delavayi, Carbohydr. Polym. 184 (2018) 127–134.

[38] R. Guo, L. Ai, N. Cao, J. Ma, Y. Wu, J. Wu, X. Sun, Physicochemical properties and structural characterization of a galactomannan from Sophora alopecuroides L. seeds, Carbohydr. Polym. 140 (2016) 451–460.

[39] H. Wang, J. Chen, P. Ren, Y. Zhang, S. Omondi Onyango, Ultrasound irradiation alters the spatial structure and improves the antioxidant activity of the yellow tea polysaccharide, Ultrason. Sonochem. 70 (2021), 105355.

[40] X.M. Wang, M. Wang, H.J. Xue, M. Zhang, D.P. Hao, R.G. Sun, A comparative study on structure and conformation of polysaccharides in ophiopogon japonicus by hot water and ultrasonic extraction, J. Instrumental Anal. 37 (2018) 23–30 (in Chinese).

[41] J. Wang, J. Wang, Y. Tang, Q. Xu, S. Huang, J. Yao, J. Zhang, Z. Lei, Regioselective sulfation of Artemisia sphaerocephala polysaccharide: Solution conformation and antioxidant activities in vitro, Carbohydr. Polym. 136 (2016) 527–536.

[42] D. Yuan, C. Li, Q. Huang, X. Fu, Ultrasonic degradation effects on the physicochemical, rheological and antioxidant properties of polysaccharide from Sargassum pallidum, Carbohydr. Polym. 239 (2020), 116230.

[43] R. Derek, M. Prentice, J.R. Stark, M.J. Gidley, Granule residues and "ghosts" remaining after heating A-type barley-starch granules in water, Carbohydr. Res. 227 (1992) 121–130.

[44] D.M.de. Carvalho, J. Berglund, Célia Marchand, M.E. Lindström, F. Vilaplana, O. Sevastyanova, Improving the thermal stability of different types of xylan by acetylation, Carbohydr. Polym. 220 (2019) 132–140.

[45] S.M. van Ruth, J.P. Roozen, Influence of mastication and saliva on aroma release in a model mouth system, Food Chem. 71 (2000) 339–345.

[46] Y. Liu, B. Zhang, S.A. Ibrahim, S.-S. Gao, H. Yang, W. Huang, Purification, characterization and antioxidant activity of polysaccharides from Flammulina velutipes residue, Carbohydr. Polym. 145 (2016) 71–77.

[47] J. Hu, Z.Y. Jin, J. Wang, Extraction and purification of inulin from Jerusalem artichoke, Food Sci. Technol. (2007) 62–65.

[48] X.-zhi. Wan, C. Ai, Y.-han. Chen, X.-xiang. Gao, R.-ting. Zhong, B. Liu, X.-hua. Chen, C. Zhao, Physicochemical Characterization of a Polysaccharide from Green Microalga Chlorella pyrenoidosa and Its Hypolipidemic Activity via Gut Microbiota Regulation in Rats, J. Agric. Food Chem. 68 (5) (2020) 1186–1197.

[49] E.N. Bergman, Energy contributions of volatile fatty acids from the gastrointestinal tract in various species, Physiol. Rev. 70 (1990) 567–590.

[50] A.J. Leonel, J.I. Alvarez-Leite, Butyrate: implications for intestinal function, Curr. Opin. Clin. Nutr. Metab. Care 15 (5) (2012) 474–479.

[51] A. Hague, B. Singh, C. Paraskeva, Butyrate acts as a survival factor for colonic epithelial cells: Further fuel for the in vivo versus in vitro debate, Gastroenterology 112 (1997) 1036–1040.

[52] P.Brøbech. Mortensen, M.R. Clausen, H. Bonnén, H. Hove, K. Holtug, Colonic fermentation of ispaghula, wheat bran, glucose, and albumin to short-chain fatty acids and ammonia evaluated in vitro in 50 subjects, J. Parenter. Enter. Nutr. 16 (5) (1992) 433–439.

[53] Y.-X. Yang, Z.-L. Dai, W.-Y. Zhu, Important impacts of intestinal bacteria on utilization of dietary amino acids in pigs, Amino Acids 46 (11) (2014) 2489–2501.

[54] L. Szablewski, Human Gut Microbiota in Health and Alzheimer's Disease, J. Alzheimers Dis. 62 (2) (2018) 549–560.

[55] P.J. Turnbaugh, R.E. Ley, M.A. Mahowald, V. Magrini, E.R. Mardis, J.I. Gordon, An obesity-associated gut microbiome with increased capacity for energy harvest, Nature 444 (2006) 1027–1031.

[56] A. Koliada, G. Syzenko, V. Moseiko, L. Budovska, K. Puchkov, V. Perederiy, Y. Gavalko, A. Dorofeyev, M. Romanenko, S. Tkach, L. Sineok, O. Lushchak, A. Vaiserman, Association between body mass index and Firmicutes/Bacteroidetes ratio in an adult Ukrainian population, BMC Microbiol. 17 (1) (2017), https://doi.org/10.1186/s12866-017-1027-1.

[57] N.R. Shin, T.W. Whon, J.W. Bae, Proteobacteria: microbial signature of dysbiosis in gut microbiota, Trends Biotechnol. 33 (2015) 496–503.

[58] Petia Kovatcheva-Datchary Anne Nilsson Rozita Akrami Ying Shiuan Lee Filipe De Vadder Tulika Arora Anna Hallen Eric Martens Inger Björck Fredrik Bäckhed Dietary fiber-induced improvement in glucose metabolism is associated with increased abundance of Prevotella Cell Metab. 22 6 2015 971 982.

[59] Y. Ding, Y. Yan, Y. Peng, D. Chen, J. Mi, L. Lu, Q. Luo, X. Li, X. Zeng, Y. Cao, In vitro digestion under simulated saliva, gastric and small intestinal conditions and fermentation by human gut microbiota of polysaccharides from the fruits of Lycium barbarum, Int. J. Biol. Macromol. 125 (2019) 751–760.

[60] L. Zhu, S.S. Baker, C. Gill, W. Liu, R. Alkhouri, R.D. Baker, S.R. Gill, Characterization of gut microbiomes in nonalcoholic steatohepatitis (NASH) patients: A connection between endogenous alcohol and NASH, Hepatology 57 (2013) 601–609.

[61] J. Zhang, Z. Guo, Z. Xue, Z. Sun, M. Zhang, L. Wang, G. Wang, F. Wang, J. Xu, H. Cao, H. Xu, Q. Lv, Z. Zhong, Y. Chen, S. Qimuge, B. Menghe, Y. Zheng, L. Zhao, W. Chen, H. Zhang, A phylo-functional core of gut microbiota in healthy young Chinese cohorts across lifestyles, geography and ethnicities, Isme J. 9 (9) (2015) 1979–1990.

[62] D. Ríos-Covián, P. Ruas-Madiedo, A. Margolles, M. Gueimonde, C.G. de los Reyes-Gavilán, N. Salazar, Intestinal short chain fatty acids and their link with diet and human health, Front. Microbiol. 7 (2016), https://doi.org/10.3389/fmicb.2016.00185.

[63] S. Xiao, C. Liu, M. Chen, J. Zou, Z. Zhang, X. Cui, S. Jiang, E. Shang, D. Qian, J. Duan, Scutellariae radix and coptidis rhizoma ameliorate glycolipid metabolism of type 2 diabetic rats by modulating gut microbiota and its metabolites, Appl. Microbiol. Biotechnol. 104 (1) (2020) 303–317.

[64] E.M. Clayton, M.C. Rea, F. Shanahan, E. Quigley, B. Kiely, C. Hill, R.P. Ross, The vexed relationship between Clostridium difficile and inflammatory bowel disease: an assessment of carriage in an outpatient setting among patients in remission, Am. J. Gastroenterol. 104 (2009) 1162.

[65] S. Lang, A. Martin, F. Farowski, H. Wisplinghoff, M.J.G.T. Vehreschild, J. Liu, M. Krawczyk, A. Nowag, A. Kretzschmar, J. Herweg, B. Schnabl, X.M. Tu, F. Lammert, T. Goeser, F. Tacke, K. Heinzer, P. Kasper, H. Steffen, Münevver Demir, High protein intake is associated with histological disease activity in patients with NAFLD, Hepatol. Commun. 4 (5) (2020) 681–695.

[66] L. Wang, R. Cheng, X. Sun, Y. Zhao, W. Ge, Y. Yang, Y. Gao, Z. Ding, J. Liu, J. Zhang, Preparation and gut microbiota modulatory property of the oligosaccharide riclinoctaose, J. Agric. Food Chem. 69 (12) (2021) 3667–3676.

[67] P. Lukova, M. Nikolova, E. Petit, R. Elboutachfaiti, C. Delattre, Prebiotic activity of poly- and oligosaccharides obtained from Plantago major L. leaves, Appl. Sci.-Basel 10 (2020) 2648.

[68] Y. Liao, T. Wu, W. Zhang, G. Gu, C. Lu, G. Wu, Effects of acidolysis and enzymolysis products of fenugreek polysaccharide on growth of intestinal flora in vitro, Sci. Technol. Food Ind. 28 (2007) 4.

[69] C.J. Chang, C.S. Lin, C.C. Lu, J. Martel, Y.F. Ko, D.M. Ojcius, S.F. Tseng, T.R. Wu, Y. Chen, J.D. Young, Ganoderma lucidum reduces obesity in mice by modulating the composition of the gut microbiota, Nat. Commun. 6 (2017) 7489.